RAPID COMMUNICATIONS

PHYSICAL REVIEW E VOLUME 52, NUMBER 6 DECEMBER 1995

Collimation of an intense laser beam by a weakly relativistic plasma

P. Monot, T. Auguste, P. Gibbon,* F. Jakober, and G. Mainfray

Commissariat à l'Energie Atomique, DSM/DRECAM/SPAM, Bâtiment 522, Centre d'Etudes de Saclay, 91191 Gif-sur-Yvette Cedex, France

(Received 15 June 1995)

We present an experimental investigation of the propagation of a 1-ps-terawatt laser pulse in a hydrogen gas jet. A study of the output beam profile shows that beam divergence is significantly reduced when laser power is close to—*but lower than*—the critical power for relativistic self-focusing. It is shown that this effect depends dramatically on the gas used.

PACS number(s): 52.35.Mw, 52.40.Db, 42.50.Rh

Numerous works have been devoted to the study of extended propagation of laser beams in nonlinear media, mainly in liquids or solids [1,2]. New short pulse lasers provide powers in excess of the terawatt level and focused intensities as high as 10^{18} W/cm^2 [3,4]. When such an intense pulse is focused onto a gaseous target, a plasma is created in the rising edge of the pulse by optical-field ionization (OFI) of the gas. The quiver velocity of freed electrons in the laser field then becomes relativistic. The resulting laser-induced electron mass increase leads to a new source of nonlinearity that can result in self-focusing of the laser in the plasma [5,6]. This effect is of special interest because it overcomes the limitation in intensity imposed by conventional focusing means, lenses or mirrors. It could also increase interaction lengths. This is a very interesting feature for new concepts of particle accelerator [7] or x-ray lasers [8]. Furthermore, relativistic self-focusing is a self-effect and is consequently expected to occur using a simple experimental arrangement with no need of an additional tailoring laser beam.

Since relativistic self-focusing arises from an electron inertia increase under the action of the intense traveling em wave, the plasma frequency ω_p is modified. The refractive index of the plasma n is then given by

$$\left(1-\frac{N_e}{\gamma N_c}\right)^{1/2}, \tag{1}$$

where γ is the relativistic factor and N_e and N_c are the electronic and the critical density, respectively ($N_c = 10^{21}$ cm^{-3} for $\lambda = 1053$ nm). The index profile with a maximum on-axis is then analogous to a positive lens. This effect can be amplified by the electron departure from the center of the beam under the action of the ponderomotive force. Numerous theoretical studies have been devoted to this subject and give a critical power P_c for self-focusing. The expression generally admitted is [5,6]

$$P_c(\mathrm{W}) = 2\times 10^{10}\times\frac{N_c}{N_e}. \tag{2}$$

It has to be emphasized that this critical power does not represent a threshold power but rather an equilibrium power for which natural diffraction is exactly balanced by nonlinear terms. For laser powers commonly achieved at present (i.e., the TW level), this corresponds to an electron density which can be obtained with a gas target ionized with the laser itself. The major difficulty is to overcome defocusing arising from laser-induced electron density gradients [9]. This can be done by using a jet which allows the laser to be focused at the entrance of the gaseous medium [11]. In this paper, we present an experimental study of the propagation in a gas undergoing ionization for laser power below the critical power given by Eq. (2).

The Saclay terawatt laser system, used in the present experiment, has been extensively described elsewhere [10]. It is based on chirped pulse amplification in Nd:glass rods followed by temporal compression. Energies up to 1.5 J can be obtained for $\lambda = 1053$ nm and for a 1-ps pulse duration. A 10^{18} W/cm^2 peak intensity is reached in vacuum [4]. The linearly polarized laser beam is focused with a $f/5$ plano-convex lens at the entrance of a hydrogen pulsed jet (Fig. 1). The neutral gas density measured with a Wollaston interferometer has a 1×3 mm flat-top profile. The laser propagates along the 3-mm length. Hydrogen is ionized in the leading edge of the pulse as soon as the laser intensity exceeds 10^{14} W/cm^2 [12]. Most of the pulse then experiences a fully

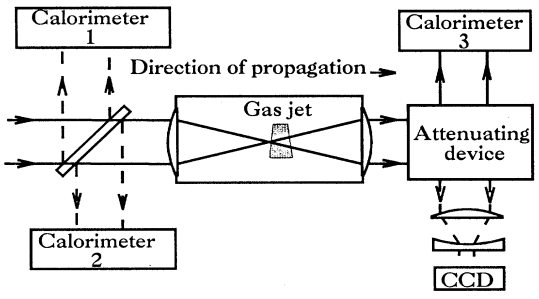

FIG. 1. Experimental setup. The laser is focused at the entrance of a pulsed hydrogen gas jet. Calorimeters 1, 2, and 3 measure the incident, the backscattered, and the transmitted energy respectively. The output beam is imaged onto a CCD camera after attenuation.

*Present address: Max-Planck-Gesellschaft, Research Unit X-Ray Optics, University of Jena, D-07743 Jena, Germany.

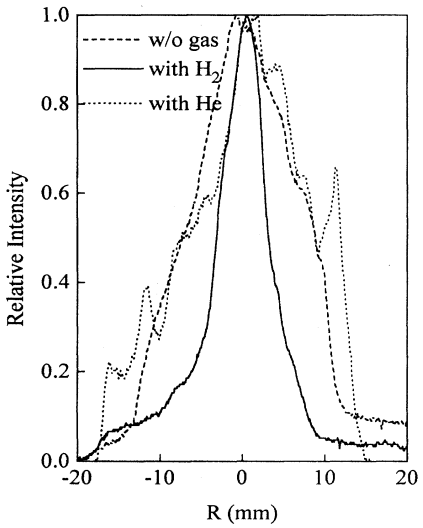

FIG. 2. Single shot measurement of far-field laser intensity profile obtained for $P=0.7$ TW with H_2 (solid line), with He (dotted line) and without gas (dashed line). The laser is focused at the jet entrance. $N_e=10^{19}$ cm^{-3}. x-axis units are in the object plane.

ionized medium consisting only of protons and electrons. The electron density gradients resulting from ionization are expelled in the leading edge and in the far wings of the pulse. Thus, only a small amount of the beam is defocused. The electron density is determined by measuring the Raman shifted component in the spectrum of the backscattered light [13]. A 10^{19} cm^{-3} maximum density is achieved in these experiments. The output beam is collimated by a lens and attenuated by successive glass reflections. The far-field intensity profile is then imaged onto a charged-coupled-device (CCD) camera after being reduced by a factor of 6. Because the laser is focused at the jet entrance, the beam waist position and spot size are fixed and variations in the far-field profile width provide a direct measurement of changes in beam divergence angle induced by the plasma. The detection system resolution is estimated to be 90 μm. The main part of the pulse is sent toward calorimeter 3 (see Fig. 1) that measures the transmitted energy. A pickup plate is set before the interaction chamber to monitor the incident energy and to measure the percentage of backscattered light. The fraction of incident and backscattered energy reflected by the glass plate (4%) is measured by calorimeters 1 and 2, respectively.

A single shot measurement of the output beam profile is shown in Fig. 2 without gas (dashed line), with H_2 (solid line), and with He (dotted line). The intensity profiles, normalized to the peak value, are obtained for a laser power of 0.7 TW and for a 10^{19} cm^{-3} electron density. The units for the x axis are given in the object plane. One can see a large reduction in the beam radius after the laser has propagated through the 3-mm-length of the plasma. As previously mentioned, because of a fixed beam waist position and spot size, this feature on the far-field intensity profile may be interpreted as a plasma-induced reduction in the beam divergence angle. It is reduced here by a factor of 2.1. This factor is obtained by applying the $1/e^2$ criterion for intensity to a Gaussian fit of profiles shown in Fig. 2. The beam shape remains quite smooth after propagating through the plasma. There is no modulation in the profile—at least on the scale length allowed by the detection system resolution—which would be a signature of a filamentation of the beam.

One must emphasize that this beam divergence reduction is observed for laser power *below* the critical power required for self-focusing. In the case mentioned above, the ratio of the incident power to the critical power is equal to 0.3. A crude estimate of the beam divergence can be obtained using a simple ray equation with a first order nonlinear term. This approximation is well justified as long as the laser power remains below the critical power and for a weakly relativistic intensity (i.e., for $I \ll I_C$ where I_C is the Compton intensity, $I_C=2.5\times10^{18}$ W/cm^2 for $\lambda=1053$ nm and for a linearly polarized wave; here $I/I_C\approx0.2$). After simple calculations, the ray equation—describing the evolution of a Gaussian beam radius along the propagation direction—is given by [14]

$$\frac{R^2}{R_0^2}=\left(1-\frac{P}{P_c}\right)\frac{2z^2}{k^2R_0^4}\left[1+\frac{z}{R_0}\left(\frac{dR}{dz}\right)_{z=0}\right]^2, \tag{3}$$

where R is the $1/e^2$ beam radius, $R_0=R(z=0)$ is the initial radius, and k is the laser wave vector. When the laser is focused at the entrance of the jet $[(dR/dz)_{z=0}=0]$, the ratio of the beam divergence in a weakly relativistic plasma to that in vacuum is given, far from the focus, by

$$\frac{\theta}{\theta_0}=\left(1-\frac{P}{P_c}\right)^{1/2}. \tag{4}$$

For $P=P_c/3$ the beam should be reduced by a factor of 1.2 instead of the factor of 2.1 measured experimentally. However, owing to the simplicity of the calculation, the above equation gives quite a good estimate of the observed beam divergence reduction.

A more detailed calculation has been performed using a steady-state propagation model [15]—similar to that described in Ref. [16]—based on a standard paraxial wave equation. In this model, one assumes that the electron response to the laser excitation is adiabatic and ions are treated as a neutralizing background. Figure 3 shows the $1/e^2$ Gaussian beam radius evolution along the propagation axis for focal geometry, laser and plasmas parameters relevant to our experimental conditions ($P=0.7$ TW, $N_e=10^{19}$ cm^{-3}). The laser is focused at the entrance of a radially homogeneous profile. The position along the propagation axis is measured from the focus position. The curve drawn with the dashed line corresponds to the case of a pulse propagating in vacuum while the solid line shows the beam radius evolution modified by the plasma. In this case, one can observe a clear reduction of the beam divergence whereas the focal spot size remains unchanged. The reduction is again less marked in the numerical calculation than in the experiment. The $1/e^2$ width of the far-field profile is 1.3 times smaller than that calculated for vacuum diffraction (see the inset of Fig. 3). In order to match our observations, the ratio P/P_c must be increased by a factor of 2 in the numerical calculation. This discrepancy cannot result from the uncertainty on the laser power is only 20%. This could come from an overestimate of

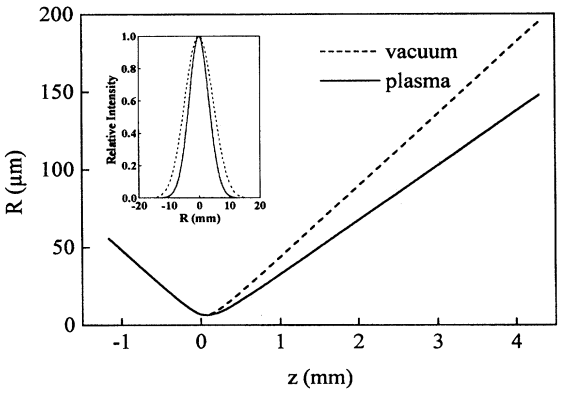

FIG. 3. Numerical calculation of the $1/e^2$ beam radius evolution along the propagation direction for $P=0.7$ TW and $N_e=10^{19}$ cm^{-3}. The laser is focused at the entrance of the 3-mm plasma. The inset shows the far-field intensity profile calculated with (solid line) and without (dashed line) plasma.

the critical power given by Eq. (2). Our experimental results would be consistent with a critical power given by

$$P_c(\mathrm{W})=10^{10}\times\frac{N_c}{N_e}, \tag{5}$$

which differs by a factor of 2 from the expression by Eq. (2). However, previous experiments performed with a shorter pulse duration laser ($\tau\sim 300$ fs) [3] and for power exceeding the critical power show that relativistic self-focusing does indeed occur for the value given by Eq. (2) [17]. In the present experiment, the reduction of the critical power for self-focusing could be due to the ion departure from the center of the beam under the action of the space-charge force. The space-charge field resulting from the ponderomotive drift of electrons is given by [18]

$$E=-\frac{m_e c^2}{q}\nabla_\perp \gamma, \tag{6}$$

where m is the electron mass, c is the light velocity, $-q$ is the charge of the system, and $\nabla_\perp$ is the radial component of the gradient.

The characteristic time required for ions to move on a fraction of the focal spot radius w_0 under the action of the space-charge force is [17,18]

$$\Delta t_i=\frac{2\pi w_0 c}{q}\left(\frac{m_e m_i \varepsilon_0 c}{2I\lambda^2}\right)^{1/2}; \tag{7}$$

here $m_i=m_p$, the proton mass. In the present experiment, the characteristic time of motion is of the order of the pulse duration ($\Delta t_i\approx 1$ ps) while in the experiment described in Ref. [17], the pulse duration is at least three times shorter than Δt_1. Ion departure should lead to a more drastic electron cavitation inducing a reduction of the critical power for self-focusing.

We must emphasize that most of the incident laser energy remains trapped into the small output beam spot. The energy after interaction has been measured as high as 80% of the incident energy. The beam narrowing induced by the plasma gives rise to an increase of the laser intensity on output optics by a factor of 3.5 causing damage for higher laser power. The 20% energy lost can be partitioned as 1% into the OFI process, 1% into stimulated Raman backscatter (RBS), and 18% into OFI-induced defocusing and stimulated Raman forward scatter (RFS). We did not measure yet the respective importance of these two latter processes. However, it is clear that the losses due to RFS are well below those measured by Coverdale *et al.* [19] for experimental conditions close to ours. We think that the influence of RFS on the beam propagation may be somewhat diminished by focusing at the gas entrance, i.e., the additional refraction due to instabilities acts on a beam which is already diverging.

Finally, beam divergence reduction depends crucially on the gas used to create the plasma. When helium is used instead of hydrogen, the far-field intensity profile, obtained for $N_e=10^{19}$ cm^{-3}, shows that the beam is broken into several filaments. The resulting strongly modulated profile is shown in Fig. 2 by the dotted line. The dramatic change induced in the propagation when using helium instead of hydrogen may be explained by the large laser intensity required to fully ionize helium ($I\approx 2\times 10^{16}$ W/cm^2, i.e., two orders of magnitude larger than for hydrogen [20]). Consequently, one can no longer consider that the plasma is created in the leading edge and in the far wings of the pulse. Beam defocusing—induced by radial electron density gradients due to OFI of the gas—must take place. However, the percentage of transmitted energy remains around 70% which is almost twice the value measured in gas-cell experiments [9]. This may be explained by (i) the smaller extension of the medium used here and (ii) the position of the focus. Note that for the same reasons, nonlinearities induced by the gas observed by others [21] in gas-cell experiments and for laser intensity close to ionization threshold should also be significantly reduced.

In conclusion, a reduction in beam divergence appears for lower power close to—*but lower than*—the critical power for self-focusing generally accepted. For $P=0.7P_c$ the beam divergence is reduced by a factor of 2.1 after interaction. Numerical calculations describing the laser propagation and taking into account the plasma response to the ponderomotive force give a reduction of beam divergence which remains smaller than the one observed experimentally. Our observation would match numerical simulations for a critical power half the one generally admitted. It is pointed out that this discrepancy could be due to the ion motion which is not taken into account in the numerical model and which can take place on the 1-ps pulse duration. When the pulse is focused into hydrogen, 80% of the incident laser energy remains near Gaussian in shape while the use of helium leads to strong modulations into the output beam profile. A possible explanation may be the residual effect of OFI which induces modulations into the plasma refraction index via the production of He^+ and He^{2+} ions. This result suggests that ionization dynamics plays a crucial role in the propagation of laser pulses with intensity well beyond the gas ionization threshold intensity.

[1] G. A. Askar'yan, Zh. Éksp. Theor. Fiz. **42**, 1567 (1962) [Sov. Phys. JETP **15**, 1088 (1962)].
[2] Y. R. Shen, Prog. Quantum Electron. **4**, 3 (1975).
[3] C. Rouyer *et al.*, Opt. Lett. **18**, 214 (1993).
[4] D. Normand *et al.*, Opt. Lett. **15**, 1400 (1990).
[5] C. E. Max, J. Arons, and A. B. Langdon, Phys. Rev. Lett. **33**, 209 (1974); G. Schmit and W. Horton, Comments Plasma Phys. Controlled Fusion **9**, 85 (1985); D. C. Barnes, T. Kurki-Suono, and T. Tajima, IEEE Trans. Plasma Sci. **15**, 154 (1987); P. Sprangel, C. M. Tang, and E. Esarey, *ibid.* **15**, 145 (1987); G. Z. Sun, E. Ott, Y. C. Lee, and P. Guzdar, Phys. Fluids **30**, 526 (1987).
[6] A. B. Borisov *et al.*, Phys. Rev. Lett. **68**, 2309 (1992).
[7] E. Esarey *et al.*, Phys. Fluids B **5**, 2690 (1993).
[8] D. C. Eder *et al.*, Phys. Plasmas **1**, 1744 (1994).
[9] P. Monot *et al.*, J. Opt. Soc. Am. B. **9**, 1579 (1992); T. Auguste *et al.*, Opt. Common. **89**, 145 (1992).
[10] M. Ferray *et al.*, Opt. Commun. **75**, 278 (1990).
[11] T. Auguste *et al.*, Opt. Commun. **105**, 292 (1994).
[12] C. Cornaggia *et al.*, Phys. Rev. A **34**, 207 (1986).
[13] M. D. Perry, C. Darrow, C. Coverdale, and J. K. Crane, Opt. Lett. **17**, 523 (1992).
[14] Y. R. Shen, *The Principles of Non-linear Optics* (Wiley, New York, 1984).
[15] P. Gibbon *et al.*, Phys. Plasmas **2**, 1305 (1995).
[16] A. B. Borisov *et al.*, Phys. Rev. Lett. **65**, 1753 (1990).
[17] P. Monot *et al.*, Phys. Rev. Lett. **74**, 2953 (1995).
[18] W. B. Mori *et al.*, Phys. Rev. Lett. **60**, 1298 (1988).
[19] C. A. Coverdale *et al.*, Phys. Rev. Lett. **74**, 4659 (1995).
[20] T. Auguste *et al.*, J. Phys. B: At. Mol. Opt. Phys. **25**, 4181 (1992).
[21] C. W. Siders *et al.* (unpublished).